Impact of Localization Errors on Wireless Channel Prediction in Mobile Robotic Networks

Yuan Yan and Yasamin Mostofi

Abstract— **In this paper we are interested in understanding and mathematically characterizing the impact of localization errors on wireless channel prediction in mobile robotic networks. We take the increase of the channel prediction error variance due to localization errors as our metric and analyze it in different communication environments. In particular, we show that this metric is monotonically increasing with respect to the path loss exponent and/or the standard deviation of shadowing, and is monotonically decreasing with respect to the standard deviation of multipath. Moreover, this metric is monotonically increasing with respect to the decorrelation distance of shadowing when it (the decorrelation distance of shadowing) is small, and is monotonically decreasing with respect to it when it is large. We also briefly discuss how the localization errors in the positioning of the channel a priori samples affect the estimation of the channel underlying parameters. Finally, we verify our mathematical analysis in a simulation environment.**

I. Introduction

One fundamental issue that arises in unmanned autonomous networks is the need for assessing the link quality at unvisited locations for the purpose of task planning. Traditionally, disk models have been utilized for this purpose in the robotics literature [1], [2]. A disk model, however, is a considerable over-simplification of a wireless channel, which has motivated more recent work on realistic channel modeling and prediction in the context of robotic networks [3]–[5]. In [6], [7], we have proposed a wireless channel prediction framework that allows the robot to predict the channel quality at unvisited locations based on a small number of a priori-collected channel samples in the same environment. In practice, the true position of the robot could be different from its estimation during the operation due to localization errors [8]–[11]. This can then impact channel prediction and the corresponding planning quality, an area that requires further investigation. In this paper, we are then interested in mathematically characterizing the impact of localization errors on the performance of our channel prediction framework.

In this context, there are two different sources of localization errors. The first one is from the phase where the robot (or a team of robots) gathers a priori channel samples in the environment, which will be used for the purpose of channel prediction. In this case, the positions of the channel samples can be corrupted by localization errors, resulting in additional errors in both estimating the underlying channel parameters and predicting the channel quality at unvisited locations. The second source is from the phase where the robot plans its destination based on the predicted channel quality at an unvisited location. However, due to localization errors, it stops elsewhere in the workspace. Thus, the true value of the channel at where it stops can be further away from the predicted channel due to the additional localization errors.

In Section III, we mainly focus on the second source of localization errors and assume that the positions of the a priori channel samples are perfectly measured and the channel parameters are perfectly estimated. Fig. 1 shows our considered scenario. The robot has used our probabilistic channel prediction framework to predict the channel quality at a desired position (q), and decided to move to this position. However, due to localization errors, the robot has stopped somewhere else in the workspace ($q + \Delta q$). Since the robot has planned its task and resource allocation based on the prediction quality at position q, it is then our goal to understand how different the prediction of the channel at the desired position is from the real channel quality at the true final position. In particular, the impact of localization errors depends on the communication environment. For instance, Fig. 1 shows a sample channel in the environment with its different components marked. It can be seen that the impact of localization errors could vary significantly depending on the channel. Hence, in this section we characterize how this impact varies in different environments and as a function of channel parameters.

We take the increase in the channel prediction error variance due to localization errors as our metric. Then, we analyze how it changes in different communication environments. In particular, we mathematically show that this metric is monotonically increasing with respect to the path loss exponent and/or the standard deviation of the shadowing component of the channel, and is monotonically decreasing with respect to the standard deviation of the multipath fading component of the channel. Moreover, this metric is monotonically increasing with respect to the decorrelation distance of shadowing when it (shadowing decorrelation distance) is small, and monotonically decreasing with respect to it when it is large. Our simulation results further confirm the theoretical analysis. In Section IV, we then briefly discuss the case where the positions of the channel samples are corrupted by localization errors as well, and show how this

Yuan Yan and Yasamin Mostofi are with the Department of Electrical and Computer Engineering, University of California, Santa Barbara, CA, USA (email:{yuanyan,ymostofi}@ece.ucsb.edu).

This work was supported in part by the NSF CAREER award number 0846483.

affects the estimation of the underlying channel parameters.

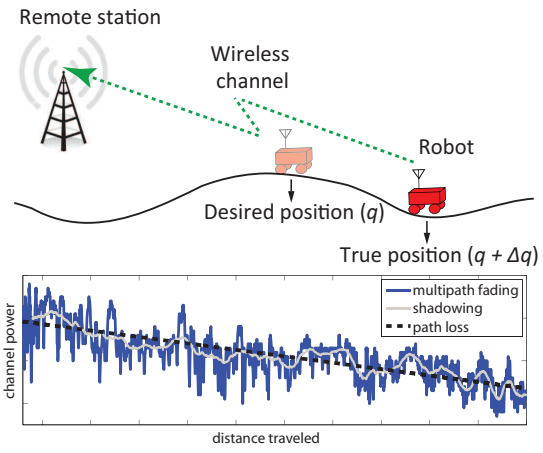

Fig. 1. Based on predicting the channel quality, the mobile robot has planned to move to some desired position (q) at which it will communicate with the remote station. However, due to localization errors, the robot has stopped at ($q+\Delta q$). Our goal is to understand how different the predicted channel quality at the desired position is from the real channel quality at the true final position.

II. A Summary of the Probabilistic Modeling and Prediction of a Wireless Channel [6], [7]

In this section we briefly summarize our previously-proposed wireless channel prediction framework that allows the robot to predict the channel quality at unvisited locations based on a small number of a priori-collected channel samples in the same environment.

As shown in the communication literature [12], the received Channel to Noise Ratio (CNR) can be modeled as a multi-scale random process with three components: path loss, shadow fading (shadowing) and multipath fading. Let $\gamma(q)$ denote the received CNR in the transmission from the remote station to the robot at position q. By using a 2D non-stationary random field model, we have the following characterization for $\gamma(q)$ (in dB): $\gamma_{\text{dB}}(q) = \alpha_{\text{PL,dB}} - 10\, n_{\text{PL}} \log_{10}\big(\|q-q_b\|\big) + \gamma_{\text{SH}}(q) + \gamma_{\text{MP}}(q)$, where $\gamma_{\text{dB}}(q) = 10\log_{10}\big(\gamma(q)\big)$, q_b is the position of the remote station, $\alpha_{\text{PL,dB}}$ and n_{PL} are the path loss parameters, and $\gamma_{\text{SH}}(q)$ and $\gamma_{\text{MP}}(q)$ are independent random variables representing the effects of shadowing and multipath fading in dB respectively [12]. In this part, we briefly summarize how the robot can probabilistically assess the spatial variations of the instantaneous received CNR, using a small number of a priori CNR measurements in the same environment.

Let $\mathcal{Q} = \{q_1, \cdots, q_m\}$ denote the set of the positions corresponding to the small number of the a priori CNR measurements available to the robot, where m represents the total number of a priori samples. Consider the ideal case of no localization errors in identifying the positions of these samples for now. The stacked vector of the received CNR measurements (in dB) can then be expressed by $Y_{\mathcal{Q}} = H_{\mathcal{Q}}\theta + \omega_{\text{SH},\mathcal{Q}} + \omega_{\text{MP},\mathcal{Q}}$, where $H_{\mathcal{Q}} = [\mathbf{1}_m \;\; -D_{\mathcal{Q}}]$, $\mathbf{1}_m$ denotes the m-dimensional vector of all ones, $D_{\mathcal{Q}} = \big[10\log_{10}(\|q_1-q_b\|) \;\cdots\; 10\log_{10}(\|q_m-q_b\|)\big]^{\text{T}}$, $\theta_{\text{PL}} = [\alpha_{\text{PL,dB}} \;\; n_{\text{PL}}]^{\text{T}}$, $\omega_{\text{SH},\mathcal{Q}} = \big[\gamma_{\text{SH}}(q_1) \;\cdots\; \gamma_{\text{SH}}(q_m)\big]^{\text{T}}$ and $\omega_{\text{MP},\mathcal{Q}} = \big[\gamma_{\text{MP}}(q_1) \;\cdots\; \gamma_{\text{MP}}(q_m)\big]^{\text{T}}$. Based on the commonly-used lognormal distribution for shadowing and its reported exponential spatial correlation [12], $\omega_{\text{SH},\mathcal{Q}}$ is a zero-mean Gaussian random vector with the covariance matrix $\Omega_{\mathcal{Q}} \in \mathbb{R}^{m\times m}$, where $\big[\Omega_{\mathcal{Q}}\big]_{i,j} = \xi^2_{\text{dB}} \exp(-\|q_i-q_j\|/\beta)$ for $i,j \in \{1,\cdots,m\}$, with ξ^2_{dB} and β denoting the variance of the shadowing component in dB and its decorrelation distance respectively. Let ρ^2_{dB} represent the power of multipath fading component (in dB) and I_m be the m-dimensional identity matrix. We have the following lemma for estimating the underlying model parameters:

Lemma 1 ([6], [7]): Define $\chi \triangleq \xi^2_{\text{dB}} + \rho^2_{\text{dB}}$. Then, the Least Square (LS) estimation of the channel parameters is given as follows: $\hat{\theta}_{\text{PL}} = (H^{\text{T}}_{\mathcal{Q}}H_{\mathcal{Q}})^{-1}H^{\text{T}}_{\mathcal{Q}}Y_{\mathcal{Q}}$, $\hat{\chi} = Y^{\text{T}}_{H_{\mathcal{Q}}}Y_{H_{\mathcal{Q}}}/m$, $\hat{\theta}_{\text{SH}} = (J^{\text{T}}_{\mathcal{Q}}WJ_{\mathcal{Q}})^{-1}J^{\text{T}}_{\mathcal{Q}}W\phi$, $\hat{\rho}^2_{\text{dB}} = \hat{\chi} - \hat{\xi}^2_{\text{dB}}$, where $Y_{H_{\mathcal{Q}}} = \big(I_m - H_{\mathcal{Q}}(H^{\text{T}}_{\mathcal{Q}}H_{\mathcal{Q}})^{-1}H^{\text{T}}_{\mathcal{Q}}\big)Y_{\mathcal{Q}}$ and $\hat{\theta}_{\text{SH}} = \big[\ln(\hat{\xi}^2_{\text{dB}}) \;\; 1/\hat{\beta}\big]^{\text{T}}$. Furthermore, $J_{\mathcal{Q}} = \big[\mathbf{1}_{|\mathcal{L}_{\mathcal{Q}}|} \;\; -G_{\mathcal{Q}}\big]$, $G_{\mathcal{Q}} = \big[l_1 \;\cdots\; l_{|\mathcal{L}_{\mathcal{Q}}|}\big]^{\text{T}}$ and $\phi = \big[\ln(\hat{r}(l_1)) \;\cdots\; \ln(\hat{r}(l_{|\mathcal{L}_{\mathcal{Q}}|}))\big]^{\text{T}}$, where $\hat{r}(l) = \big(\sum_{(i,j)\in\mathcal{A}(l)}\big[Y_{H_{\mathcal{Q}}}\big]_i\big[Y_{H_{\mathcal{Q}}}\big]_j\big)/|\mathcal{A}(l)|$ is the numerical estimation of the spatial correlation at distance l, with $\mathcal{A}(l) = \big\{(i,j) \;\big|\; q_i,q_j \in \mathcal{Q}, \big\|q_i-q_j\big\| = l\big\}$, and $\mathcal{L}_{\mathcal{Q}} = \{l \,|\, 0 < \hat{r}(l) < \hat{\chi}\} = \{l_1,\cdots,l_{|\mathcal{L}_{\mathcal{Q}}|}\}$ is the ordered set of acceptable possible distances among the samples. Finally, W is a constant weight matrix that can be chosen based on the assessment of the accuracy of the estimation of $\hat{r}(l)$.

Then, based on the measurements available to the robot and conditioned on the channel parameters, the assessment of the received CNR at an unvisited position q is given by the following lemma (assuming no localization error for q):

Lemma 2 ([6], [7]): A Gaussian random variable, $\Upsilon_{\text{dB}}(q)$, with mean $\overline{\Upsilon}_{\text{dB}}(q) = \mathbb{E}\big\{\Upsilon_{\text{dB}}(q) \;\big|\; Y_{\mathcal{Q}},\theta_{\text{PL}},\beta,\xi_{\text{dB}},\rho_{\text{dB}}\big\}$ and variance $\sigma^2_{\text{dB}}(q) = \mathbb{E}\Big\{\big(\Upsilon_{\text{dB}}(q)-\overline{\Upsilon}_{\text{dB}}(q)\big)^2\big|Y_{\mathcal{Q}},\theta_{\text{PL}},\beta,\xi_{\text{dB}},\rho_{\text{dB}}\Big\}$ can best characterize the path loss and shadowing components of CNR at q, where

$$\overline{\Upsilon}_{\text{dB}}(q) = \underbrace{H_q\,\theta_{\text{PL}}}_{\text{predicted path loss}} + \underbrace{\Psi^{\text{T}}_{\mathcal{Q}}(q)\Phi^{-1}_{\mathcal{Q}}\big(Y_{\mathcal{Q}} - H_{\mathcal{Q}}\theta_{\text{PL}}\big)}_{\text{predicted shadowing}}, \quad (1)$$

$$\sigma^2_{\text{dB}}(q) = \xi^2_{\text{dB}} + \rho^2_{\text{dB}} - \Psi^{\text{T}}_{\mathcal{Q}}(q)\Phi^{-1}_{\mathcal{Q}}\Psi_{\mathcal{Q}}(q), \quad (2)$$

$H_q = \big[1 \;\; -10\log_{10}(\|q-q_b\|)\big]$, $\Phi_{\mathcal{Q}} = \Omega_{\mathcal{Q}} + \rho^2_{\text{dB}}I_m$ and $\Psi_{\mathcal{Q}}(q) = \xi^2_{\text{dB}}\big[\exp(-\|q-q_1\|/\beta) \cdots \exp(-\|q-q_m\|/\beta)\big]^{\text{T}}$.

Then, the robot substitutes the estimated parameters of the channel (acquired from Lemma 1) in $\overline{\Upsilon}_{\text{dB}}(q)$ and $\sigma^2_{\text{dB}}(q)$ of Lemma 2 to assess the variations of the CNR in the workspace. It should be noted that this framework does not attempt to predict the multipath fading component of the channel since it typically decorrelates very fast. It rather assumes an uncorrelated Gaussian $\omega_{\text{MP},\mathcal{Q}}$. The readers are referred to [6], [7] for more details on the performance of this framework with real data and in different environments.

III. Impact of Localization Errors on Channel Prediction

Let q denote an unvisited position where the robot has predicted the channel quality to be $\overline{\Upsilon}_{\text{dB}}(q)$. Based on the

overall sensing and communication objective of the robot, it has decided to move to this location, as shown in Fig. 1. Due to the localization errors, however, the robot moves to a different position $\widetilde{q} = q + \Delta q$, where Δq is a random vector denoting the localization error. As a result, the true CNR after the robot reaches $\widetilde{q}$ is $\gamma_{\text{dB}}(\widetilde{q})$ while the robot has used the prediction at position q to plan its overall task.

As discussed earlier, in this section we assume that the positions of the a priori channel samples (q_is) are not corrupted by localization errors but the position q, where these a priori measurements are used to predict the channel, is corrupted by a localization error.[1] We further assume that the underlying channel parameters are perfectly estimated. We then relax these assumptions in the next section. Finally, we assume that the operation environment is small enough such that the underlying parameters have not changed from q to $\widetilde{q}$. Given the scale with which the underlying parameters may change, as compared to the size of localization errors, this assumption should be valid for most scenarios [7]. We next mathematically characterize the impact of localization errors on the channel prediction quality.

Consider the variance of the channel prediction error in the presence of localization errors:

$$\begin{aligned}
\sigma^2_{\text{dB},e}(\widetilde{q}) &= \mathbb{E}_{\text{C}}\Big\{\big(\overline{\Upsilon}_{\text{dB}}(q) - \gamma_{\text{dB}}(\widetilde{q})\big)^2\Big\} \\
&= \mathbb{E}_{\text{C}}\Big\{\big(\overline{\Upsilon}_{\text{dB}}(q) - \overline{\Upsilon}_{\text{dB}}(\widetilde{q}) + \overline{\Upsilon}_{\text{dB}}(\widetilde{q}) - \gamma_{\text{dB}}(\widetilde{q})\big)^2\Big\} \\
&= \mathbb{E}_{\text{C}}\Big\{\big(H_q\,\theta_{\text{PL}} - H_{\widetilde{q}}\,\theta_{\text{PL}} + \big(\Psi_{\mathcal{Q}}(q) - \Psi_{\mathcal{Q}}(\widetilde{q})\big)^{\text{T}} \\
&\qquad \times \Phi_{\mathcal{Q}}^{-1}(\omega_{\text{SH},\mathcal{Q}} + \omega_{\text{MP},\mathcal{Q}}) + \overline{\Upsilon}_{\text{dB}}(\widetilde{q}) - \gamma_{\text{dB}}(\widetilde{q})\big)^2\Big\} \\
&= \xi^2_{\text{dB}} + \rho^2_{\text{dB}} - \Psi^{\text{T}}_{\mathcal{Q}}(\widetilde{q})\Phi^{-1}_{\mathcal{Q}}\Psi_{\mathcal{Q}}(\widetilde{q}) + \big((H_q - H_{\widetilde{q}})\theta_{\text{PL}}\big)^2 \\
&\qquad + \big(\Psi_{\mathcal{Q}}(q) - \Psi_{\mathcal{Q}}(\widetilde{q})\big)^{\text{T}}\Phi^{-1}_{\mathcal{Q}}\big(\Psi_{\mathcal{Q}}(q) - \Psi_{\mathcal{Q}}(\widetilde{q})\big) \\
&= \sigma^2_{\text{dB}}(\widetilde{q}) + E_{\text{tot}},
\end{aligned}$$

where $H_{\widetilde{q}} = \big[1 \quad -10\log_{10}(\|\widetilde{q} - q_b\|)\big]$, $\Psi_{\mathcal{Q}}(\widetilde{q}) = \xi^2_{\text{dB}}\big[\exp(-\|\widetilde{q} - q_1\|/\beta) \;\cdots\; \exp(-\|\widetilde{q} - q_m\|/\beta)\big]^{\text{T}}$, $\mathbb{E}_{\text{C}}\{\cdot\}$ denotes the expectation that is taken over the realizations of the wireless channels, $\sigma^2_{\text{dB}}(\widetilde{q}) = \xi^2_{\text{dB}} + \rho^2_{\text{dB}} - \Psi^{\text{T}}_{\mathcal{Q}}(\widetilde{q})\Phi^{-1}_{\mathcal{Q}}\Psi_{\mathcal{Q}}(\widetilde{q})$ (see Lemma 2) is the variance of the channel prediction error at $\widetilde{q}$ if there was no localization error and

$$E_{\text{tot}} = \underbrace{\big((H_q - H_{\widetilde{q}})\theta_{\text{PL}}\big)^2}_{\substack{E_{\text{PL}}\text{: impact of localization errors on} \\ \text{the path loss component of channel prediction}}} + \underbrace{\big(\Psi_{\mathcal{Q}}(\widetilde{q}) - \Psi_{\mathcal{Q}}(q)\big)^{\text{T}}\Phi^{-1}_{\mathcal{Q}}\big(\Psi_{\mathcal{Q}}(\widetilde{q}) - \Psi_{\mathcal{Q}}(q)\big)}_{\substack{E_{\text{SH}}\text{: impact of localization errors on} \\ \text{the shadowing component of channel prediction}}}. \quad (3)$$

It can be seen that E_{tot} is the increase in the prediction error variance (in addition to $\sigma^2_{\text{dB}}(\widetilde{q})$) due to localization errors.

[1]This, for instance, could be the case if the robots that collected the a priori measurements have a better localization capabilities than the robot that is using the measurements for prediction and navigation. Another possible scenario is the case where the a priori measurements are collected in the part of the operation space that is more navigable (less localization errors) than the place where the robot is planning to go to.

Remark 1: Note that E_{tot}, E_{PL} and E_{SH} are functions of Δq. Thus, given the distribution of Δq, the average performance (averaged over Δq) can be found as: $\overline{E}_{\text{tot}} = \overline{E}_{\text{PL}} + \overline{E}_{\text{SH}}$. For the sake of mathematical simplicity, we carry out our analysis on E_{tot}, E_{PL} and E_{SH}, i.e. for a given Δq. But all the results clearly hold for the case where the metrics are averaged over a distribution for Δq.

It can be seen that (3) is non-negative, i.e. localization errors always degrade the channel prediction performance. Moreover, the right hand side of (3) contains two separate terms. The first term E_{PL} is the impact of localization errors on the path loss component while the second term E_{SH} is the impact of localization errors on the shadowing component (see (1)). In this part, we then mathematically characterize the impact of different environments (in terms of their underlying parameters) on E_{tot}, which is the increase of the prediction error variance due to localization errors.

A related metric is the percentage increase of the prediction variance, i.e. $E_{\text{tot}}/\sigma^2_{\text{dB}}(\widetilde{q})$. In most applications, the channel prediction is used for the purpose of planning of resources such as communication energy consumption. Thus, another useful metric is the impact of localization errors on how off the assessment of the needed resources will be. Let $\mu_{\text{pred}}(q) = f\big(\overline{\Upsilon}_{\text{dB}}(q), \sigma^2_{\text{dB}}(q)\big)$ be the prediction of the needed resources at position q, which is a function of the estimated mean and variance of the predicted channel through function $f(\cdot)$. Then, the mismatch in the prediction of the needed resources can be expressed as $\mathbb{E}_{\text{C}}\{|\mu_{\text{pred}}(q) - \mu_{\text{true}}(\widetilde{q})|\}$, where $|\cdot|$ represents the absolute value and $\mu_{\text{true}}(\widetilde{q})$ is the actual needed resources at $\widetilde{q}$. In [13], for instance, it was shown that the predicted minimum average communication energy required to satisfy a given Bit Error Rate (BER) is related to the predicted channel quality at position q as follows: $\mu_{\text{pred}}(q) = C_1 \exp\big(C_2\sigma^2_{\text{dB}}(q)\big)/\overline{\Upsilon}(q)$, where $\overline{\Upsilon}(q) = 10^{\overline{\Upsilon}_{\text{dB}}(q)/10}$, C_1 is a constant depending on the target BER and the utilized spectral efficiency, and $C_2 = (\ln 10/10)^2/2$ (see [13] for more details). Then, the mismatch in the prediction of the needed energy will be $\mathbb{E}_{\text{C}}\big\{|C_1 \exp\big(C_2\sigma^2_{\text{dB}}(q)\big)/\overline{\Upsilon}(q) - C_1/\gamma(\widetilde{q})|\big\}$, where $\gamma(\widetilde{q}) = 10^{\gamma_{\text{dB}}(\widetilde{q})/10}$. Due to the page limitations, in this paper we focus on the characterization of E_{tot}. Exploring the impact of the localization errors on other related metrics is then a possible extension of this work.

A. Impact of Localization Errors in Different Communication Environments

Next, we characterize the impact of localization errors in different communication environments.

Lemma 3: E_{PL} and consequently E_{tot} are monotonically increasing with respect to the path loss exponent n_{PL}. Moreover, if the distance between q and the remote station $\|q - q_b\|$ is considerably larger than the norm of the localization error $\|\Delta q\|$, then E_{PL} and consequently E_{tot} are monotonically decreasing with respect to $\|q - q_b\|$.

Proof: It can be easily seen that $E_{\text{PL}} = n^2_{\text{PL}}\big(10\log\big(\|\widetilde{q} - q_b\|/\|q - q_b\|\big)\big)^2$. Hence, E_{PL} and E_{tot} are monotonically increasing with respect to n_{PL}.

Moreover, if the distance between q and the remote station $\|q-q_b\|$ is considerably larger than the norm of the localization error $\|\Delta q\|$, we have the following second-order approximation for E_{PL}: $E_{\text{PL}} \approx n_{\text{PL}}^2(10\log(e))^2\Delta q^{\text{T}}(q-q_b)(q-q_b)^{\text{T}}\Delta q/\|q-q_b\|^4 = n_{\text{PL}}^2(10\log(e))^2\Delta q^{\text{T}}u_{q-q_b}u_{q-q_b}^{\text{T}}\Delta q/\|q-q_b\|^2$, where u_{q-q_b} denotes the unit vector pointing from q to q_b. As can be seen, E_{PL} and E_{tot} are monotonically decreasing with respect to $\|q-q_b\|$. ■

Intuitively, if the path loss exponent n_{PL} is larger, the path loss component of the channel varies more significantly. The first part of Lemma 3 then says that the impact of localization errors increases as n_{PL} increases. Moreover, from the path loss model, we know that the path loss component changes more significantly as the distance between q and q_b becomes smaller. The second part of Lemma 3 then says that the impact of localization errors decreases as the distance between q and q_b increases.

Lemma 4: 1) Consider the case that $\xi_{\text{dB}}^2 > 0$ and $\beta > 0$. Then, E_{SH} and consequently E_{tot} are monotonically decreasing with respect to the variance of the multipath fading (ρ_{dB}^2);

2) Consider the case that $\beta > 0$. Then, E_{SH} and consequently E_{tot} are monotonically increasing with respect to the variance of the shadowing (ξ_{dB}^2).

Proof: 1) By taking the first-order derivative of E_{SH} with respect to ρ_{dB}^2, we have $\partial E_{\text{SH}}/\partial\rho_{\text{dB}}^2 = -\big(\Psi_{\mathcal{Q}}(\widetilde{q}) - \Psi_{\mathcal{Q}}(q)\big)^{\text{T}}\Phi_{\mathcal{Q}}^{-2}\big(\Psi_{\mathcal{Q}}(\widetilde{q}) - \Psi_{\mathcal{Q}}(q)\big) < 0$, which confirms the first part of the lemma.

2) Similarly, by taking the first-order derivative of E_{SH} with respect to ξ_{dB}^2, we have $\partial E_{\text{SH}}/\partial\xi_{\text{dB}}^2 = (1/\xi_{\text{dB}}^2)\big(\Psi_{\mathcal{Q}}(\widetilde{q}) - \Psi_{\mathcal{Q}}(q)\big)^{\text{T}}\Phi_{\mathcal{Q}}^{-1}\big(\Psi_{\mathcal{Q}}(\widetilde{q}) - \Psi_{\mathcal{Q}}(q)\big) + (\rho_{\text{dB}}^2/\xi_{\text{dB}}^2)\big(\Psi_{\mathcal{Q}}(\widetilde{q}) - \Psi_{\mathcal{Q}}(q)\big)^{\text{T}}\Phi_{\mathcal{Q}}^{-2}\big(\Psi_{\mathcal{Q}}(\widetilde{q}) - \Psi_{\mathcal{Q}}(q)\big) > 0$, which confirms the second part of the lemma. ■

As mentioned in Section II, the multipath fading component of the channel is unpredictable. Intuitively, as ρ_{dB}^2 increases, we expect that the impact of localization errors decreases since the channel becomes more unpredictable even without localization errors. Part 1 of Lemma 4 confirms this. On the other hand, the shadowing component of the channel is predictable. Part 2 of Lemma 4 then says that the impact of localization errors on the shadowing component increases as ξ_{dB}^2 increases. Thus, the shadowing and multipath fading variances have opposite effects on the impact of localization errors on channel prediction.

Lemma 5: If $\beta \to 0$ or $\beta \to \infty$, then $E_{\text{SH}} \to 0$.

Proof: Clearly if $\beta \to 0$, $\Psi_{\mathcal{Q}}(\widetilde{q}) = \Psi_{\mathcal{Q}}(q) = 0$. Similarly, if $\beta \to \infty$, $\Psi_{\mathcal{Q}}(\widetilde{q}) = \Psi_{\mathcal{Q}}(q) = \mathbf{1}_m$. Therefore, we have $E_{\text{SH}} \to 0$ if $\beta \to 0$ or $\beta \to \infty$. ■

As the shadowing component of the channel becomes uncorrelated, i.e. $\beta \to 0$, there will be no corresponding shadowing component to predict any more, resulting in $E_{\text{SH}} \to 0$. On the other hand, as the shadowing component becomes fully correlated, i.e. $\beta \to \infty$, the shadowing component is the same at both q and $\widetilde{q}$. Then, we expect E_{SH} to go to 0.

Lemma 6: Define R as follows:

$$R = \Omega_{\mathcal{Q}} \bullet \big(\mathbf{1}_m \text{col}\{\|q-q_i\|\}^{\text{T}} + \text{col}\{\|q-q_i\|\}\mathbf{1}_m^{\text{T}} - T_{\mathcal{Q}}\big),$$

where $\text{col}\{\|q-q_i\|\} = \big[\|q-q_1\| \cdots \|q-q_m\|\big]^{\text{T}}$, $\bullet$ represents the Hadamard product, and matrix $T_{\mathcal{Q}} \in \mathbb{R}^{m\times m}$ has the following form: $\big[T_{\mathcal{Q}}\big]_{i,j} = \|q_i - q_j\|$. Then, we have $R \succeq 0$.

Proof: See [7] for the details of the proof. ■

While Lemma 5 characterizes two asymptotic cases, the following lemma further explores the monotonic behavior of E_{tot} with respect to β when β is small or large.

Lemma 7: Consider the case that $\xi_{\text{dB}}^2 > 0$ and $\rho_{\text{dB}}^2 > 0$. Assume that the norm of the localization error $\|\Delta q\|$ is small as compared to β and as compared to $\|q-q_i\|$ for all i. Then, there exists $\underline{\beta} > 0$ and $\overline{\beta} > 0$, such that E_{SH} and consequently E_{tot} are monotonically increasing with respect to β if $\beta \in (0, \underline{\beta})$, and are monotonically decreasing with respect to β if $\beta \in (\overline{\beta}, \infty)$.

Proof: The first-order derivative of E_{SH} with respect to β is given as follows:

$$\begin{aligned}\frac{\partial E_{\text{SH}}}{\partial\beta} = \frac{2}{\beta^2}\big(\Lambda\{\|\widetilde{q}-q_i\|\}\Psi_{\mathcal{Q}}(\widetilde{q}) - \Lambda\{\|q-q_i\|\}\Psi_{\mathcal{Q}}(q)\big)^{\text{T}} \\ \times \Phi_{\mathcal{Q}}^{-1}\big(\Psi_{\mathcal{Q}}(\widetilde{q}) - \Psi_{\mathcal{Q}}(q)\big) \\ - \frac{1}{\beta^2}\big(\Psi_{\mathcal{Q}}(\widetilde{q}) - \Psi_{\mathcal{Q}}(q)\big)^{\text{T}}\Phi_{\mathcal{Q}}^{-1}(\Omega_{\mathcal{Q}} \bullet T_{\mathcal{Q}})\Phi_{\mathcal{Q}}^{-1} \\ \times \big(\Psi_{\mathcal{Q}}(\widetilde{q}) - \Psi_{\mathcal{Q}}(q)\big),\end{aligned}$$

where $\Lambda\{a_i\}$ denotes the diagonal matrix with entries a_i on its diagonal and $T_{\mathcal{Q}}$ is defined in Lemma 6. Based on the assumption that $\|\Delta q\|$ is small as compared to β and as compared to $\|q-q_i\|$, we then have the following approximations:

$$\Delta\Psi_{\mathcal{Q}}(q) = \Psi_{\mathcal{Q}}(\widetilde{q}) - \Psi_{\mathcal{Q}}(q) \approx -\Lambda\left\{\frac{(q-q_i)^{\text{T}}\Delta q}{\beta\|q-q_i\|}\right\}\Psi_{\mathcal{Q}}(q),$$

and

$$\begin{aligned}&\Lambda\{\|\widetilde{q}-q_i\|\}\Psi_{\mathcal{Q}}(\widetilde{q}) - \Lambda\{\|q-q_i\|\}\Psi_{\mathcal{Q}}(q) \\ &\approx \Lambda\left\{\frac{(q-q_i)^{\text{T}}\Delta q}{\|q-q_i\|}\right\}\Psi_{\mathcal{Q}}(q) - \Lambda\left\{\frac{(q-q_i)^{\text{T}}\Delta q}{\beta}\right\}\Psi_{\mathcal{Q}}(q) \\ &= \big(\Lambda\{\|q-q_i\|\} - \beta I_m\big)\Delta\Psi_{\mathcal{Q}}(q).\end{aligned}$$

We then have the following second-order approximation for $\partial E_{\text{SH}}/\partial\beta$:

$$\frac{\partial E_{\text{SH}}}{\partial\beta} \approx \frac{1}{\beta^2}\big(\Delta\Psi_{\mathcal{Q}}(q)\big)^{\text{T}}\Phi_{\mathcal{Q}}^{-1}M\Phi_{\mathcal{Q}}^{-1}\Delta\Psi_{\mathcal{Q}}(q),$$

where $M = \Lambda\{\|q-q_i\|\}\Phi_{\mathcal{Q}} + \Phi_{\mathcal{Q}}\Lambda\{\|q-q_i\|\} - \Omega_{\mathcal{Q}} \bullet T_{\mathcal{Q}} - 2\beta\Phi_{\mathcal{Q}} = R + 2\rho_{\text{dB}}^2\Lambda\{\|q-q_i\|\} - 2\beta\Phi_{\mathcal{Q}}$. Clearly, a sufficient condition to guarantee the monotonicity of $\partial E_{\text{SH}}/\partial\beta$ is to ensure that M is positive definite or negative definite.

From Lemma 6, we know that R is positive semi-definite. Thus, a sufficient condition to guarantee that $M \succ 0$ is $\rho_{\text{dB}}^2 \min_i \|q-q_i\| - \beta\lambda_{\max}(\Phi_{\mathcal{Q}}) > 0$, where $\lambda_{\max}(\cdot)$ denotes the largest eigenvalue of the argument. By using Gershgorin disk theorem [14], we have

$$\lambda_{\max}(\Phi_{\mathcal{Q}}) \le \rho_{\text{dB}}^2 + \xi_{\text{dB}}^2 \max_{i\in\{1,\cdots,m\}} \sum_{j=1}^{m} \exp(-\|q_i - q_j\|/\beta),$$

where the upper bound is monotonically decreasing with respect to β. Then, there must exist a sufficiently small $\underline{\beta} > 0$ such that $\rho_{\text{dB}}^2 \min_i \|q - q_i\| - \beta\lambda_{\max}(\Phi_{\mathcal{Q}}) > 0$ for $\overline{\beta} \in (0, \underline{\beta})$. Therefore, there exists a $\underline{\beta} > 0$ such that E_{SH} and consequently E_{tot} are monotonically increasing with respect to β for $\beta \in (0, \underline{\beta})$. Similarly, we have

$$\begin{aligned}\lambda_{\max}(R) &\leq \xi_{\text{dB}}^2 \max_{i\in\{1,\cdots,m\}} \sum_{j=1}^{m} \exp\left(-\|q_i - q_j\|/\beta\right) \\ &\quad \times \left(\|q - q_i\| + \|q - q_j\| - \|q_i - q_j\|\right) \\ &\leq \xi_{\text{dB}}^2 \max_{i\in\{1,\cdots,m\}} \sum_{j=1}^{m} \|q - q_i\| + \|q - q_j\| - \|q_i - q_j\|,\end{aligned}$$

i.e. $\lambda_{\max}(R)$ is bounded from above by a constant. Then, there must exist a sufficiently large $\overline{\beta}$ such that $M \prec 0$. As a result, we have E_{SH} and consequently E_{tot} monotonically decreasing with respect to β for $\beta \in (\overline{\beta}, \infty)$. ■

B. Simulation Results

Consider the case where the remote station is located at the origin, and the desired position q is $(10\text{ m}, 10\text{ m})$. Δq is chosen as a zero mean Gaussian random variable with covariance matrix I_2. Our simulation results are averaged over 100 realizations of wireless channels generated using our probabilistic channel simulator [15]. Also, for each realization of the channel, the results are averaged over 2000 realizations of Δq.

Fig. 2 (left) shows the impact of localization errors on channel prediction quality for different path loss exponents. Other channel parameters are chosen as follows: $\alpha_{\text{PL,dB}} = -50$, $\xi_{\text{dB}} = 4$ and $\beta = 10$ m. Moreover, multipath fading is chosen as Rician fading with parameter $K_{\text{ric}} = 20$. As can be seen, the impact increases as the path loss exponent increases (see Lemma 3). Fig. 2 (right) shows the impact of localization errors on channel prediction quality for different standard deviations of the shadowing component. Other channel parameters are chosen as follows: $\alpha_{\text{PL,dB}} = -50$, $n_{\text{PL}} = 3$ and $\beta = 10$ m. Moreover, multipath fading is chosen as Rician fading with parameter $K_{\text{ric}} = 5$. It can be seen that the impact increases as the standard deviation of shadowing increases, as proved in the second part of Lemma 4.

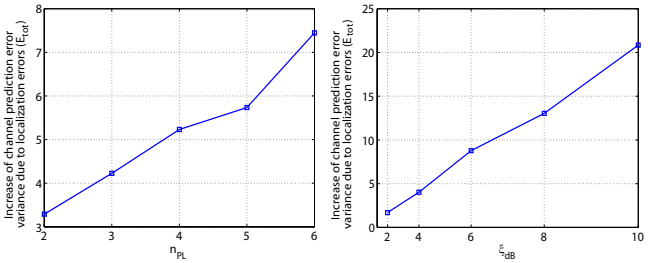

Fig. 2. Impact of localization errors on channel prediction quality for different path loss exponents (left) and for different standard deviations of the shadowing component (right). As can be seen, the impact increases as the path loss exponent increases (see Lemma 3). Also, the impact increases as the standard deviation increases (see the second part of Lemma 4).

Fig. 3 (left) shows the impact of localization errors on channel prediction quality for different standard deviations of the multipath fading component. Multipath fading is chosen as Rician fading with parameter K_{ric}. Then, the standard deviation increases as K_{ric} decreases. Other channel parameters are chosen as follows: $\alpha_{\text{PL,dB}} = -50$, $n_{\text{PL}} = 3$, $\beta = 10$ m and $\xi_{\text{dB}} = 4$. It can be seen that the impact decreases as the standard deviation of multipath fading increases, as proved in the first part of Lemma 4. Finally, Fig. 3 (right) shows the impact of localization errors on channel prediction quality for different decorrelation distances of the shadowing component. Other channel parameters are chosen as follows: $\alpha_{\text{PL,dB}} = -50$, $n_{\text{PL}} = 3$ and $\xi_{\text{dB}} = 8$. Moreover, multipath fading is chosen as Rician fading with parameter $K_{\text{ric}} = 5$. As can be seen, the impact of localization errors increases as the decorrelation distance increases for small β, while the impact decreases as the decorrelation distance increases for large β (see Lemma 7).[2]

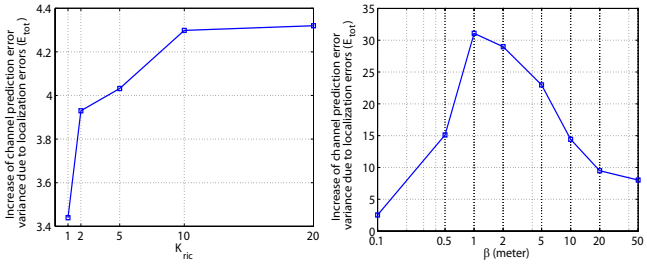

Fig. 3. Impact of localization errors on channel prediction quality for different standard deviations of the multipath fading component (left) and for different decorrelation distances of the shadowing component (right). As can be seen, the impact increases as the standard deviation decreases (see the first part of Lemma 4). Also, the impact increases as the decorrelation distance increases for small β, while the impact decreases as the decorrelation distance increases for large β (see Lemma 7). Note that the standard deviation increases as K_{ric} decreases.

IV. Impact of the Localization Errors on Channel Parameter Estimation

In this part, we extend our previous scenario and consider the case where the positions of the a priori channel samples are also corrupted by the localization errors. We then analyze how the localization errors affect the channel parameter estimation.

Let $\widetilde{\mathcal{Q}} = \{\widetilde{q}_1, \cdots, \widetilde{q}_m\}$ denote the set of the true positions where the a priori channel samples are measured, with $\widetilde{q}_i = q_i + \Delta q_i$, for $i \in \{1, \cdots, m\}$, and Δq_i denoting the localization error of the position of the i^{th} sample. Also, let $Y_{\widetilde{\mathcal{Q}}}$ represent the stacked vector of the corresponding channel measures. Then, the LS estimation of the path loss parameter is given by: $\hat{\theta}_{\text{PL},e} = (H_{\mathcal{Q}}^{\text{T}} H_{\mathcal{Q}})^{-1} H_{\mathcal{Q}}^{\text{T}} Y_{\widetilde{\mathcal{Q}}}$ (see Lemma 1), which results in the following Mean Square Error (MSE):

$$\begin{aligned}\mathbb{E}_{\text{C}}\left\{\|\hat{\theta}_{\text{PL},e} - \theta_{\text{PL}}\|^2\right\} &= n_{\text{PL}}^2 \|(H_{\mathcal{Q}}^{\text{T}} H_{\mathcal{Q}})^{-1} H_{\mathcal{Q}}^{\text{T}} (D_{\widetilde{\mathcal{Q}}} - D_{\mathcal{Q}})\|^2 \\ &\quad + \text{tr}\left\{(H_{\mathcal{Q}}^{\text{T}} H_{\mathcal{Q}})^{-1} H_{\mathcal{Q}}^{\text{T}} \Phi_{\widetilde{\mathcal{Q}}} H_{\mathcal{Q}} (H_{\mathcal{Q}}^{\text{T}} H_{\mathcal{Q}})^{-1}\right\}, \quad (4)\end{aligned}$$

where $H_{\widetilde{\mathcal{Q}}} = [\mathbf{1}_m \ -D_{\widetilde{\mathcal{Q}}}]$, $D_{\widetilde{\mathcal{Q}}} = \left[10\log_{10}(\|\widetilde{q}_1 - q_b\|) \ \cdots \ 10\log_{10}(\|\widetilde{q}_m - q_b\|)\right]^{\text{T}}$, $\omega_{\text{SH},\widetilde{\mathcal{Q}}} = \left[\gamma_{\text{SH}}(\widetilde{q}_1) \ \cdots \ \gamma_{\text{SH}}(\widetilde{q}_m)\right]^{\text{T}}$, $\omega_{\text{MP},\widetilde{\mathcal{Q}}} = \left[\gamma_{\text{MP}}(\widetilde{q}_1) \ \cdots \ \gamma_{\text{MP}}(\widetilde{q}_m)\right]^{\text{T}}$, $\Phi_{\widetilde{\mathcal{Q}}} = \Omega_{\widetilde{\mathcal{Q}}} + \rho_{\text{dB}}^2 I_m$ and $\text{tr}\{\cdot\}$ denotes the trace of the argument. Furthermore,

[2]In the simulation, we use different set of parameters for each figure to better show the impact of the corresponding channel parameter. For example, in Fig. 3 (right), we use a larger shadowing standard deviation (ξ_{dB}) to better show the impact of shadowing decorrelation distance (β).

covariance matrix $\Omega_{\widetilde{\mathcal{Q}}} \in \mathbb{R}^{m\times m}$ has the following form: $\left[\Omega_{\widetilde{\mathcal{Q}}}\right]_{i,j} = \xi_{\text{dB}}^2 \exp(-\|\widetilde{q}_i - \widetilde{q}_j\|/\beta)$ for $i,j \in \{1,\cdots,m\}$.

Note that the first term in (4) is monotonically increasing with respect to n_{PL}. This is intuitive since the path loss component of the channel varies more significantly as a function of distance when n_{PL} is larger, magnifying the impact of localization errors.

The characterization of the impact on the estimation of the shadowing parameter is more challenging. For simplicity, in the next analysis, we assume that the path loss component of the samples can be perfectly estimated. Let $\hat{r}_e(l_k)$, for $k \in \{1,\cdots,|\mathcal{L}_{\mathcal{Q}}|\}$, denote the numerical estimation of the spatial correlation of shadowing in this case. In order to calculate this, the robot chooses the set $\mathcal{A}(l_k)$ in Lemma 1 to include all the sample pairs where $\|q_i - q_j\| = l_k$, for some $i,j \in \{1,\cdots,m\}$. However, due to the localization errors in the positions of the samples, the true distance between the corresponding samples is $\widetilde{l}_k = \|\widetilde{q}_i - \widetilde{q}_j\|$. Hence, $\hat{r}_e(l_k)$ is also averaged over localization errors. Furthermore, we assume that $|\mathcal{A}(l_k)|$, for $k \in \{1,\cdots,|\mathcal{L}_{\mathcal{Q}}|\}$, is considerably large such that $\hat{r}_e(l_k)$ converges to its mean with high probability. Then, we have $\hat{r}_e(l_k) \approx \mathbb{E}_{\text{L}}\{\xi_{\text{dB}}^2 \exp(-\widetilde{l}_k/\beta)\}$, where $\mathbb{E}_{\text{L}}\{\cdot\}$ denotes the expectation taken over the localization errors. Moreover, we assume that the environment where the samples are taken is one-dimensional, and Δq_is are zero-mean independent Gaussian random variables [9] with standard deviation $\sigma_l/\sqrt{2}$, for all i. After some straightforward calculation, we have

$$\hat{r}_e(l_k) \approx \xi_{\text{dB}}^2 \exp\left(-\frac{l_k}{\beta} + \frac{\sigma_l^2}{2\beta^2}\right) \times \left[1 - Q\left(\frac{l_k}{\sigma_l} - \frac{\sigma_l}{\beta}\right) + \exp\left(\frac{2\,l_k}{\beta}\right) Q\left(\frac{\sigma_l}{\beta} + \frac{l_k}{\sigma_l}\right)\right],$$

where $Q(\cdot)$ denotes the Q function.

Consider the case where σ_l is small such that $\sigma_l \ll \min_{k\in\{1,\cdots,|\mathcal{L}_{\mathcal{Q}}|\}} \sqrt{\beta l_k}$ and $\sigma_l \ll \min_{k\in\{1,\cdots,|\mathcal{L}_{\mathcal{Q}}|\}} l_k$. Then, we have $Q\left(l_k/\sigma_l - \sigma_l/\beta\right) \approx 0$ and $\exp\left(2\,l_k/\beta\right) Q(\sigma_l/\beta + l_k/\sigma_l) < \left(1/\left(\sqrt{2\pi}(\sigma_l/\beta + l_k/\sigma_l)\right)\right) \exp\left(l_k/\beta - l_k^2/(2\sigma_l^2) - \sigma_l^2/(2\beta^2)\right) \approx 0$.

As a result, we have $\hat{r}_e(l_k) \approx \xi_{\text{dB}}^2 \exp\left(-l_k/\beta + \sigma_l^2/2\beta^2\right)$ for all k. Thus, the LS estimation of the shadowing parameters becomes

$$\begin{aligned}\hat{\theta}_{\text{SH}} &= (J_{\mathcal{Q}}^{\text{T}} W J_{\mathcal{Q}})^{-1} J_{\mathcal{Q}}^{\text{T}} W \phi_e \\ &\approx \theta_{\text{SH}} + \frac{\sigma_l^2}{2\beta^2}(J_{\mathcal{Q}}^{\text{T}} W J_{\mathcal{Q}})^{-1} J_{\mathcal{Q}}^{\text{T}} W \mathbf{1}_{|\mathcal{L}_{\mathcal{Q}}|}, \end{aligned} \quad (5)$$

where $\phi_e = \left[\ln(\hat{r}_e(l_1)) \;\cdots\; \ln(\hat{r}_e(l_{|\mathcal{L}_{\mathcal{Q}}|}))\right]^{\text{T}} \approx J_{\mathcal{Q}}\theta_{\text{SH}} + (\sigma_l^2/2\beta^2)\mathbf{1}_{|\mathcal{L}_{\mathcal{Q}}|}$.

Note that the second term in (5) is the shadowing parameters estimation error caused by the localization errors, which depends on the ratio σ_l/β. Clearly, the second term decreases as the ratio σ_l/β decreases. This means that the impact of localization errors is small (large) if the standard deviation of the localization errors is small (large) as compared to the decorrelation distance.

V. Conclusions

In this paper, we characterized the impact of localization errors on the wireless channel prediction quality. We considered the increase of the channel prediction error variance, due to localization errors, as our metric and mathematically characterized how it behaved in different communication environments. For instance, we showed that this metric is monotonically increasing with respect to the path loss exponent and/or the standard deviation of shadowing, and is monotonically decreasing with respect to the standard deviation of multipath. Moreover, this metric is monotonically increasing with respect to the decorrelation distance of shadowing when it is small, and monotonically decreasing with respect to it when it is large. We also briefly showed how the localization errors in the positioning of the a priori channel samples affect the estimation of the channel underlying parameters. We verified our analysis in a simulation environment. Considering the impact of localization errors on both the positions of the a priori samples and the final destination position of the robot is a possible future direction for this work.

References

[1] M. M. Zavlanos, M. B. Egerstedt, Y. C. Hu, and G. J. Pappas. Graph-theoretic connectivity control of mobile robot networks. *Proceedings of the IEEE*, 99(9):1525 – 1540, July 2011.

[2] Cory Dixon and Eric W. Frew. Optimizing cascaded chains of unmanned aircraft acting as communication relays. *IEEE Journal on Selected Areas in Communications*, 30(5):883–898, 2012.

[3] A. Ghaffarkhah and Y. Mostofi. Communication-aware motion planning in mobile networks. *IEEE Trans. on Automatic Control, special issue on Wireless Sensor and Actuator Networks*, 56(10):2478–2485, 2011.

[4] M. Lindhé and K. H. Johanson. Using robot mobility to exploit multipath fading. *IEEE Wireless Comm.*, 16(1):30–37, Feb. 2009.

[5] A. Ghaffarkhah and Y. Mostofi. Dynamic coverage of time-varying fading environments. *ACM Trans. on Sensor Networks*, 2013. to appear.

[6] Y. Mostofi, M. Malmirchegini, and A. Ghaffarkhah. Estimation of communication signal strength in robotic networks. In *Proc. of the 50th IEEE Int'l Conf. on Robotics and Automation*, pages 1946–1951, Anchorage, Alaska, May 2010.

[7] M. Malmirchegini and Y. Mostofi. On the spatial predictability of communication channels. *IEEE Trans. on Wireless Comm.*, 11(3):964–978, Mar. 2012.

[8] S. Thrun, W. Burgard, and D. Fox. *Probabilistic Robotics*. MIT Press, 2005.

[9] J. J. Leonard and H. F. Durrant-Whyte. *Directed Sonar Sensing for Mobile Robot Navigation*. Springer, 1992.

[10] S. Se, D. Lowe, and J. Little. Mobile robot localization and mapping with uncertainty using scale-invariant visual landmarks. *The international Journal of robotics Research*, 21(8):735–758, 2002.

[11] J. Biswas, B. Coltin, and M. Veloso. Corrective gradient refinement for mobile robot localization. In *IEEE/RSJ International Conference on Intelligent Robots and Systems (IROS)*, pages 73–78, 2011.

[12] A. Goldsmith. *Wireless Communications*. Cambridge University Press, 2005.

[13] Y. Yan and Y. Mostofi. Co-optimization of communication and motion planning of a robotic operation under resource constraints and in fading environments. *IEEE Trans. on Wireless Comm.*, 12(4):1562 – 1572, April 2013.

[14] R.A. Horn and C.R. Johnson. *Matrix analysis*. Cambridge university press, 1990.

[15] A. Gonzalez-Ruiz, A. Ghaffarkhah, and Y. Mostofi. A comprehensive overview and characterization of wireless channels for networked robotic and control systems. *Journal of Robotics*, 2011.